Three Dimensional Particle-In-Cell Simulation for the Development of Air Breathing Ion Engine

IEPC-2015-463p／ISTS-2015-b-463p

Presented at Joint Conference of 30th International Symposium on Space Technology and Science
34th International Electric Propulsion Conference and 6th Nano-satellite Symposium,
Hyogo-Kobe, Japan
July 4 – 10, 2015

Shinichiro Kawaguchi[1]
Graduate School of Engineering, Kobe University, Kobe, Hyogo, 10543, Japan

Hideyuki Usui[2], Yohei Miyake[3]
Graduate School of System Informatics, Kobe University, Kobe, Hyogo, 10543, Japan

Tsubasa Yasukouchi[4]
Graduate School of Engineering, Kobe University, Kobe, Hyogo, 10543, Japan

Masato Fukuda[5]
Graduate School of System Informatics, Kobe University, Kobe, Hyogo, 10543, Japan

and

Kumiko Yokota[6], Masahito Tagawa[7]
Graduate School of Engineering, Kobe University, Kobe, Hyogo, 10543, Japan

Abstract: Three-dimensional numerical calculations using electromagnetic spacecraft environment simulator (EMSES) were carried out for air breathing ion engine (ABIE) development. Basic properties regarding formation of the plasma were examined such as relationship between wavelength and the diameter of discharge chamber, or magnet arrangement in the discharge chamber. It was confirmed that the microwave energy was transferred to atoms at certain locations in the discharge chamber. Importance of the design guide line of ABIE for concentrating the incoming atoms/molecules to energy transfer locations is suggested.

Nomenclature

I_1	=	electron density (or intensity)
n_2	=	neutral particle density
x	=	beam direction
σ	=	cross-section of electron/neutral collision

[1] Graduate student, Department of Mechanical Engineering, 147t330t@stu.kobe-u.ac.jp
[2]Professor, Department of System Informatics, h-usui@port.kobe-u.ac.jp
[3]Assistant Professor, Department of System Informatics, y-miyake@eagle.kobe-u.ac.jp
[4]Graduate student, Department of Mechanical Engineering, 150t376t@stu.kobe-u.ac.jp
[5]Graduate student, Department of System Informatics, 1145077t@stu.kobe-u.ac.jp
[6]Resarch staff, Department of Mechanical Engineering, yokota@mech.kobe-u.ac.jp
[7]Assosiate Professor, Department of Mechanical Engineering, tagawa@mech.kobe-u.ac.jp

P_i	=	collision probability of electrons per unit time
V_i	=	velocity of the incident electron
n_t	=	neutral particle density
B	=	dipole magnetic field strength
R	=	position vector from the center of magnetic field
m_d	=	dipole moment vector
v	=	velocity of the electron
E	=	electric field strength
Δt	=	time step
B_{dipole}	=	dipole magnetic field

I. Introduction

LOWERING the orbital altitude of satellites provides many advantages for Earth observation purposes such as high-resolution imaging of Earth surface[1]. Steady sub-low Earth orbit (sub-LEO) satellites are now planned in some countries[2, 3]. European space agency pioneered by the gravity field and steady-state ocean circulation explorer (GOCE)[5]. GOCE equips very complicated thruster system to maintain the altitude at 270 km for very sensitive gravity measurement. On the other hand, Japan aerospace exploration agency will launch super-low altitude test satellite (SLATS) in 2016, which is targeting the altitude of 180km. SLATS will measure the atmospheric density, and material degradation in sub-LEO region[6]. These sub-LEO satellites must equip electric propulsion system to compensate the drag from atmosphere. The mission life will be limited by the amount of Xe propellant to be carried. This is the case of GOCE. This limitation becomes more remarkable for small satellites. In order to overcome this limitation, air breathing ion engine (ABIE) concept was proposed by Nishiyama[1]. Atoms/molecules in the upper atmosphere is compressed inside the ABIE and microwave plasma is generated with the compressed atmosphere[7]. Compression of atmosphere was achieved simply by the scattering of gas molecules by the reflector inside the ABIE inlet[8]. Therefore, the optimum design of ABIE is strongly related to the space environment in the targeted altitude.

The ground-based space environmental simulation in sub-LEO region is under investigation. Hyperthermal (8 km/s) continuous beam consisting of atomic oxygen or molecular nitrogen is needed for ABIE evaluations. However, such continuous beam is not available at this point. The only available beam is a hyperthermal beam pulses created by the laser-detonation facility, which has been used for material degradation studies in LEO[6]. In our previous study, a laser-detonation facility was used for the evaluation of ABIE[5]. It was recognized through the previous experimental study that the experimental evaluation using pulsed beam is quite difficult due to the instable phenomena of microwave-generated plasma[8, 9]. Due to the difficulty for simulating the neutral gas environment in laboratories, ABIE-related studies have been carried out theoretical or numerical basis[10,11,12]. However, experimental verification is needed for further improvement of the ABIE development.

In this study, plasma formation property inside ABIE was studied using a numerical simulation based on particle-in-cell (PIC) method for performing the experimental study of ABIE.

II. Numerical simulation method

A. Simulation method

The simulation code used in this simulation is electromagnetic spacecraft environment simulator (EMSES) which is based on the Maxwell's equations for electromagnetic fields reaction and the equation of motion for a large number of macro-particle with the FDTD scheme and the Newton's law for thermions of plasma particles. This simulation code has been developed for the self-consistent analysis of the spacecraft-plasma interactions[8]. Characteristic feature of EMSES is the time-dependent electromagnetic field update based on the kinetic plasma motions in the simulation space[13].

B. The ion generation model and the dipole moment model

Previous study developed the ion generation algorism in the EMSES based on the MCC model. The electron density in the plasma is gradually decreased by electron-atom collisions. Change in the electron density through electron-atom collision is given by the equation (1);

$$dI_1 = -\sigma I_1 n_t dx \quad (1)$$

σ is the cross-section of the electron-atom collisional reactions which depends on the collision energy. The cross-section is expressed as the function of the sum of the kinetic energy of the intake particle. The amount of the cross-section between the intake particle and the neutral particle is expressed by the sum of the cross-section for each kind of the collisions between them.

The collisional processes between electron and atoms such as ionization or scattering were categorized by the value of Pi is expressed by (2), v_1 is velocity of the incident electron, nt is neutral particle density, xi is the beam direction[14,15].

$$P_i = 1 - \exp(-\Delta t v_i \sigma n_t (x_i)) \tag{2}$$

In the EMSES, we defined dipole magnetic field given by Equation (3).

$$B_{dipole} = (3 \times \frac{md \cdot r}{r^5} \cdot r - \frac{md}{r^3}) \tag{3}$$

r is a position vector from the center of magnetic field, and md is dipole moment vector. In order to reflect magnetic field to plasma dynamics, the magnetic field distribution over the computational area was calculated. All plasma particles in the simulation space follow the magnetic field distribution in the equations of motion shown in Equation (4).

$$\frac{dv}{dt} = \frac{q}{m}(E + v \times (B + B_{dipole})) \tag{4}$$

C. Simulation model

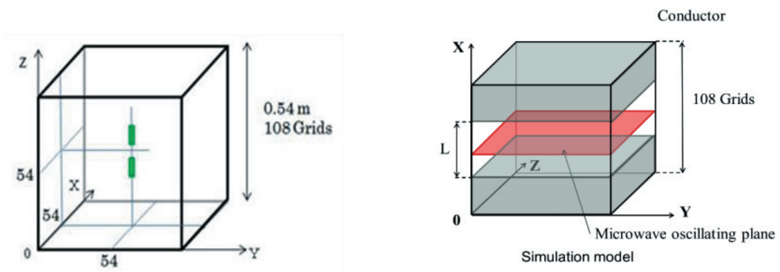

Figure 1. simulation space for the plane wave simulation (left) and the simulation model for plane wave simulation (right)

Two types of the simulations were performed in this study, which are plane wave simulation and ABIE simulation, respectively. Figure 1 shows the simulation model and the simulation space for the plane wave simulation. The simulation space consists of 108 × 108 × 108 grids. Table 1 shows the simulation parameters for the plane wave simulation. Microwave was radiated from the center plane of the simulation space (x = 54). Note that the metal boundaries were installed in the model in order to simulate the effect of metallic wall of the discharge chamber. The ABIE simulation was also performed in the simulation space in 108 × 108 × 108 grids.

Table 1. Simulation parameters for the plane wave simulation.

Parameter	value
Time step (Δ t)	1.7E-12 s
Grid spacing (l)	5E-3 m
Initial electron density (n_e)	1.7E6 m^{-3}
Initial electron velocity (v_e)	0 eV
Collision frequency (ν ')	1.0E-4 s^{-1}
Power (P)	35 W
Magnetic force (m_d)	0.027 T

The simulation model of ABIE used in this study was based on the design of experimental model used in our previous study Figure 2[5]. Figure 3 shows the cross-section of the simulation model of ABIE. The dipole antenna located at the center of discharge chamber was set in two 5-grid-long electrically conducting rods with a 2-grids spacing. The magnet configuration of the μ 6 ion engine was simulated as shown in Figure 4. Figures 4(a) and 4(b) indicate the top and cross-sectional views of the magnet arrangement. The bi-cylindrical magnets surrounding the microwave antenna are placed with the radii of 7 and 15 mm, respectively. Table 2 lists the simulation parameter fro the ABIE simulations. All calculations in this study were performed with the Kyoto-daigaku denpa-kagaku keisanki-jikken(KDK) supercomputer in Research Institute for Sustainable Humanosphere (RISH) Kyoto[9].

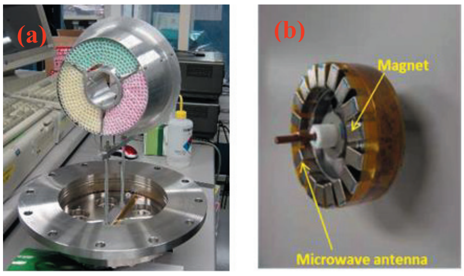

Figure 2. Experimental model of ABIE used in the previous study (left) and the μ 6 ion engine (right)

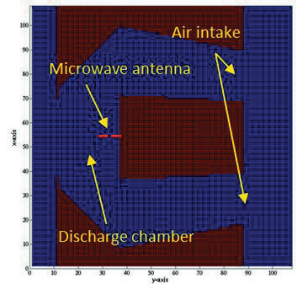

Figure 3. Cross-section of the simulation model of ABIE at z=54 plane.

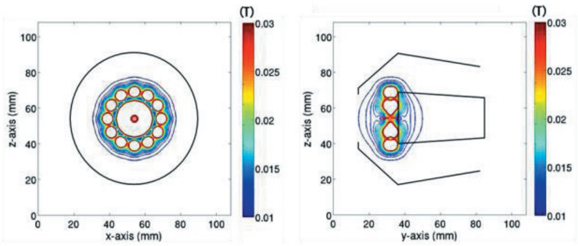

Figure 4. Magnet configuration of μ6 ion Engine. Left; top view at y=32 and, Right; side view at x=54

Table 2. Simulation parameters for the ABIE simulations.

Parameter	value
Time step (Δ t)	1.7E-12 s
Grid spacing (l)	1.0E-3 m
Initial electron density (n_e)	1.7E6 1 m^{-3}
Initial electron velocity (v_e)	0.0 eV
Collision frequency (ν ')	1.0E-4 s^{-1}
Frequency (Hz)	3 GHz
Power (P)	35 W
Magnetic force (m_d)	0.027 T

III. Results and Discussion

A. Plane Wave Simulation

A relationship between wavelength of the microwaves λ and ion generation efficiency was examined by the plane wave simulation. Figure 5. shows the electromagnetic energy transferred to electrons as a function of microwave wavelength relative to the discharge chamber diameter. It was clearly indicated that the electrons efficiently received electromagnetic energy at λ/L=0.4, 0.7 and 2.0. These are the locations satisfying the relationship of L=λ/2 × n (n=1, 2 and 3). It was confirmed that the electromagnetic energy of microwave is transferred to electrons efficiently when the standing wave was formed in the discharge chamber. However, the actual ABIE dimensions are L=6 cm for μ6 ion engine and λ= 7-12 cm for the microwave at 2.45 to 4.2 GHz. Thus, it is not realistic to use standing waves to accelerate electrons in the discharge chamber in the μ 6 ion engine.

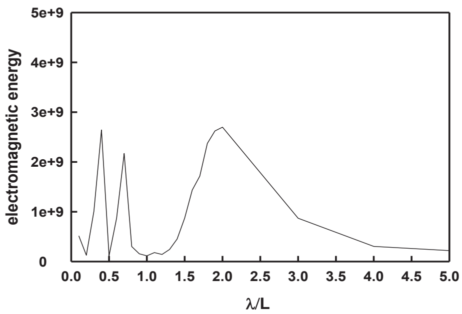

Figure 5. The electromagnetic energy transformation

B. ABIE Model Simulation

Figure6. shows the ion density distribution in the discharge chamber. It is clearly indicated that the ions are generated only at the vicinity of the microwave antenna. This computational result suggested that the standing wave was not formed in the discharge chamber, which was predicted by the plane wave simulation in the previous section. Moreover, it was calculated that the microwave energy was radiated through the inlet of the ABIE.

In order to prevent the radiation of microwave energy through the inlet, the metal reflector needs to be installed. On the other hand, atoms/molecules coming through the inlet must be focused efficiently in the discharge chamber. Combining these two requirements, a cylindrical metal mesh was introduced in the discharge chamber. The mesh can confine the microwave energy within a small domain near the antenna, while the mesh is nearly transparent for incoming atoms/molecules. Two configurations of the metal mesh were calculated by EMSES, i.e., mesh radii of 10 mm and 20 mm, and the results were compared to the case without the metal mesh. Figure 7 shows the total number of ions generated in the discharge chamber as a function of time. It is indicated that the metal mesh promotes the ion generation up to 120 % in the case of R =20 mm, while, the amount of ions generated is drastically decreased by locating the metal mesh at R = 10 mm. In order to understand the ion generation property depending on the mesh diameter, electric field distribution and electron density distributions in the discharge chamber were examined. Figures 8. (a) and (b) show the electron density distribution in the discharge chamber for R=10 and 20 mm cases, respectively. It is clearly indicated that the electron density inside the metal mesh decreased in the case of R=10 mm. Electrons are concentrated near the y=18 mm position where 10 mm downstream from the antenna. On the other hand, high-electron density region was localized near the magnet in the case of R=20 mm. This result indicated that the electrons are not trapped by the ECR region in the case of R=10mm. Figure 9 indicates the electric field distribution in the discharge chamber with R=10mm configuration. It is obvious that the high-electric field was formed not only the vicinity of the antenna, but also entire mesh region. Electrons in the mesh area are exhausted to the downstream due to the presence of strong electric field and kept away from the magnet. This considerably degrades the efficiencies of electron-atom collisions and the resulting ion generation, because electron should be accommodated near the magnet to exploit an ECR effect for efficient electron acceleration. From the results obtained in this study, it was suggested that the diameter of the metal mesh affects the electric field in side the discharge chamber of ABIE, which critically governs the performance of ABIE.

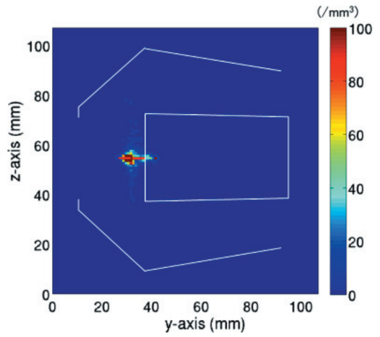

Figure 6. Spatial density distribution of ions generated in the discharge chamber.

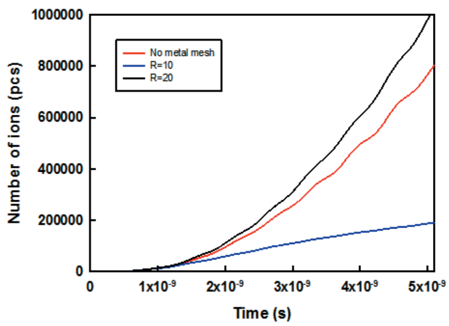

Figure 7. Number of ions generated in the discharge chamber as a function of time with metal mesh of R=10 and 20 mm.

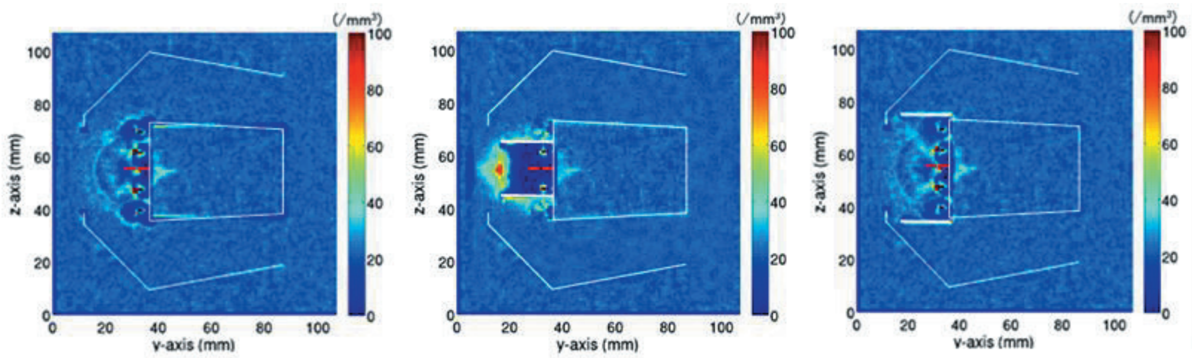

(a) (b) (c)

Figure 8. Electron density distribution in the discharge chamber (a); no mesh and (b); with metal mesh R=10 mm and (c); with R=20 mm.

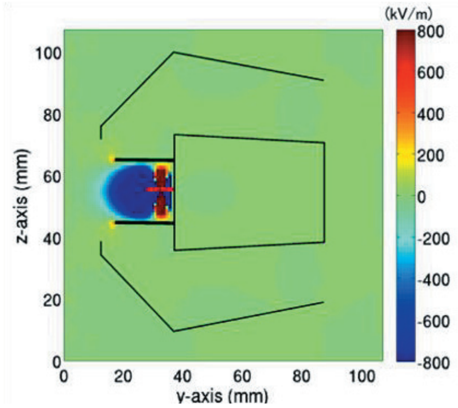

Figure 9. Spatial distribution of electric field strength in the discharge chamber with metal mesh R=10

IV. Conclusions

Numerical simulation for obtaining the optimum design of Air Breathing Ion Engine was carried out by using Electromagnetic Spacecraft Environment Simulator. From the plane wave simulation, it was calculated that the microwave energy was transferred to electrons at the position satisfying the relationship of $L=\lambda/2\times n$ (n=1, 2 and 3). This demonstrates the validity of the simulations. The simulation model based on the experimental model of ABIE was developed. It was calculated that the metal mesh installed to prevent the leaking the microwave energy through the air inlet also affect the electron density distribution inside the discharge chamber. High-performance ABIE design for a ground-based experiment is being developed based on the calculations obtained in this study.

V. Acknowledgments

The authors appreciate Mr. A. Hashimoto of Kobe University for his help with the calculation. A part of this work was supported by the Grant-in-Aids from Japan Society for Promotion of Science contract number #25289307, #26289322, 15K14252 and 15K14253. Computation in this study was carried out at the Institute for Information Management and Communication, Kyoto University.

References

[11]Nishiyama, K., “Air Breathing Ion Engine Concept” *Proceedings of the 54th International Astronautical Congress,* International Astronautical Federation, Paris, 2003; also Paper IAC-03-S4-02.

[2]Hisamoto, Y., Nishiyama, K, Kuninaka, H., “Characteristics of Hyperthermal Atomic Oxygen Source Using Electron Cyclotron Resonance Discharge and Neutralization Grid”, *Transactions of The Japan Society for Aeronautical and Space Sciences*, Aerospace Technology Japan Vol. 12, 2014, pp.43-48.

[3] Komurasaki, K., “An over view of electric propulsion activities in Japan”, *39th AIAA/ASME/SAE/ASEE Joint Propulsion Conference and Exhibit*, AIAA 2003-5272 ,2003,

[4]Hohman, K., “Atmospheric breathing electric thruster for planetary exploration," *Final Report*, 2012.

[5]Williams, N., Jjameson, P.,Sanders, C., Fehringer, M., Edwards, C., “The GOCE Ion Propulsion Assembly – Lessons Learnt from the First 22 Months of Flight Operations”, *32nd International Electric Propulsion Conference,* 2011.

[6]Tagawa, M., Kishida, K., Yokota, K., “Calibration of Atomic Oxygen Sensors adoard Satellites,” *Astronautical Science/Japan Aerospace Exploration Agency*, Space Utilize 26, 2010

[7]Hisamoto, Y., Nishiyama K. and Kuninaka, K., "Design of air intake for air breathing ion engine", Proc. 63rd Int. Astron.Congr., 2012, pp.,1, 5.

[8]Fujita, K., “Air Intake Performance of Air Breathing Ion Engine“, *Japan Society for Aeronautical and Space Sciences*, Vol.52. 2004 , pp., 514, 521.

[9]Garrigues, L., “Computational Study of Hall-Effect Thruster with Ambient Atmospheric Gas as Propellant”, *Journal of Propulsion and Power*, Vol. 28, No. 2, 2012, pp., 344, 354.

[10]Tony, S., Komurasaki, K., Francesco, R., Bartomeu, M. B., Georg Herdrich, “Analysis of atmosphere-breathing electric propulsion”, *IEEE Transactions on Plasma Science*, Vol. 43, 2015, pp., 287, 294.

[11]Motoyama, T., Usui, H., Miyake, Y., Yokota, K., Tagawa, M., “Microwave plasma simulation for the development of air breathing ion engine“, *The 29th International Space Technology and Sciences*, Nagoya, 2013.

[12]Garrigues, L., “Computational Study of Hall-Effect Thruster with Ambient Atmospheric Gas as Propellant”, *Journal of Propulsion and Power*, Vol. 28, No. 2, 2012, pp., 344, 354.

[13]Miyake Y, Usui H, “New electromagnetic particle simulation code for the analysis of spacecraft-plasma interactions“ , *Phusics of plasmas 16*, 2009, 062904.
[14]Vahedi V, Surendra M, “A Monte Carlo collision model for the particle-in-cell method“, applications to argon and oxygen discharges, *Computer Physics Communications*, Vol.87, 1995 , pp., 179, 198.
[15]Keishi, T., “ Electromagnetic Field Analysis and Its Applications to Product Development“, *Sei technichal review*, No. 69, Oct-2009, pp., 4, 12.